

Zika Virus after the Public Health Emergency of International Concern Period, Brazil

Laith Yakob

More than 100,000 Zika virus cases have been reported in Brazil since the Public Health Emergency of International Concern period ended in 2016. We analyzed cases in Brazil during 2017–2021 to identify transmission trends and forecast future infection hotspots. Our results can be used for targeted interventions to reduce transmission.

Zika virus (ZIKV) is a flavivirus transmitted through the bite of mosquitoes, principally *Aedes aegypti*. The World Health Organization (WHO) declared a Public Health Emergency of International Concern (PHEIC) on February 1, 2016, by which time autochthonous ZIKV transmission had been reported in 22 countries and territories in Latin America and the Caribbean (1). The PHEIC was prompted by the reporting 2 months earlier of a suspected link between ZIKV infection during pregnancy and subsequent birth defects, most notably microcephaly (2). A high proportion of asymptomatic or mild infections (3) coupled with diagnostic test cross-reactivity (4) obscured the true number of cases during the outbreak. Accounting for these sources of uncertainty recent modeling suggests 132.3 million (95% CI 111.3–170.2 million) persons in the Americas had been infected by the end of 2018 (5).

WHO terminated the emergency in November 2016. During the next 5 years, 2017–2021, infection rates decreased substantially; for example, the United States reported 15 new local cases in 2017 and none since (6). However, ZIKV did not disappear from the region; $\geq 150,000$ cases were reported, unadjusted for underreporting, in the Americas through September 2021 (7). The persistence of ZIKV in this region coupled with its explosive epidemic potential has meant ZIKV remains in the WHO list of priority

diseases for research and development in emergency contexts (8). We explored post-PHEIC ZIKV transmission in Brazil, the country with the highest number of infections during the epidemic in the Americas. Our first objective was to analyze post-PHEIC infection trends in Brazil; the second was to identify consistent places and times for ongoing transmission for intervention targeting.

The Study

All data were anonymized and reported at the municipality level. We obtained ZIKV infection data from the online database of the Brazilian Ministry of Health's notifiable diseases information system (Sistema de Informação de Agravos de Notificação, SINAN) (9). We used data from laboratory-confirmed (either by real-time PCR or IgM serology) and clinically diagnosed cases. (Figure 1).

We adapted an autoregressive integrated moving average model to enable direct modeling of the seasonal component of time series data. We tested our seasonal autoregressive integrated moving average (SARIMA) model on monthly cases from January 2017–December 2019 and then validated it with 2020 data before using it for forecasting for 2021–2022. Parameterization involved fitting data to alternative SARIMA models by a modified Powell method and selecting the model with lowest Akaike Information Criterion. We assumed a seasonality lag of 12 time steps (i.e., seasonality repeats every 12 months) for SARIMA models and trained and validated the model for each of the 5 regions of Brazil.

Diagnostic plots for the SARIMA models comprise the standardized residuals, normal Q-Q plot, and the correlogram; all generally indicated good model fits for the data from each region (Appendix Figures 1–5, <https://wwwnc.cdc.gov/EID/article/28/4/21-1949-App1.pdf>). For 2021–2022, we forecasted the following case numbers for each region: North, 291 (95% CI 0–5,334); Northeast, 5,933 (95% CI 251–17,009);

Author affiliation: London School of Hygiene and Tropical Medicine, London, England

DOI: <https://doi.org/10.3201/eid2804.211949>

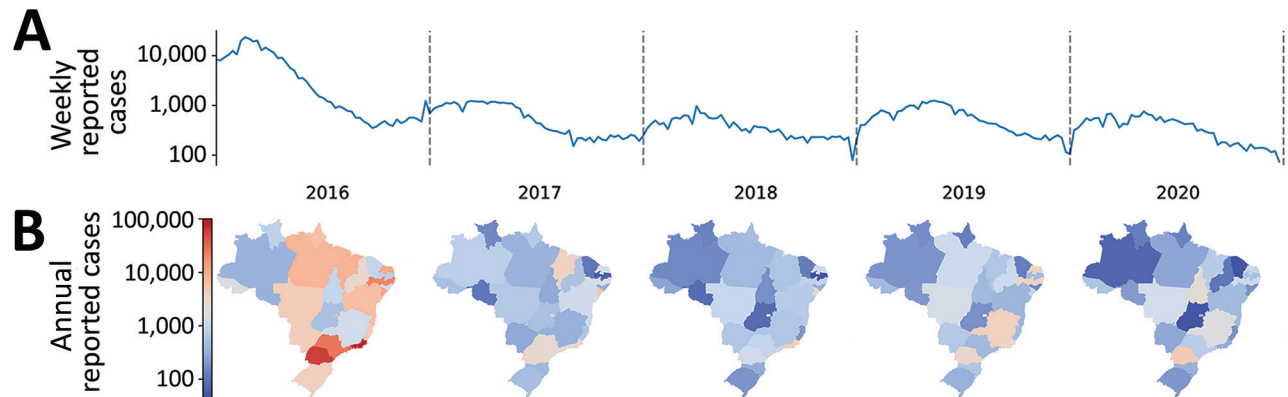


Figure 1. Weekly reported Zika cases in Brazil, 2016–2020. A) Log scale of reported cases during and after the Public Health Emergency of International Concern period, which ended in November 2016. B) State-level distribution of cases for each year, as reported to the Sistema de Informação de Agravos de Notificação (9) database (bottom).

Southeast, 1,228 (95% CI 0–21,793); South, 291 (95% CI 28–208); and Central-West, 733 (95% CI 0–10,388) (Appendix Figure 6). We recorded final model specifications and the root mean squared errors for the 2020 SARIMA predictions (Appendix).

We applied a data filter to 5,570 municipalities in Brazil, and included in our analysis those that have reported ZIKV infections consistently every year since 2017. We generated a kernel density plot (10) for these areas of consistent transmission and weighted the data by minimum annual rate of infection, standardized to local municipality population;

the latest census was >10 years ago, so we used 2020 estimates produced by the Brazilian Institute of Geography and Statistics (11). We identified centroid locations of all municipalities that reported ZIKV cases after 2016 and the hotspots of sustained transmission during the post-PHEIC period, in which ≥ 40 cases were reported per 100,000 population consistently each year (Figure 2, panel A). We generated contours from kernel density estimates weighted by the minimum annual rate of infection standardized to local municipality population. We noted hotspots in Roraima and Tocantins (North region), Alagoas

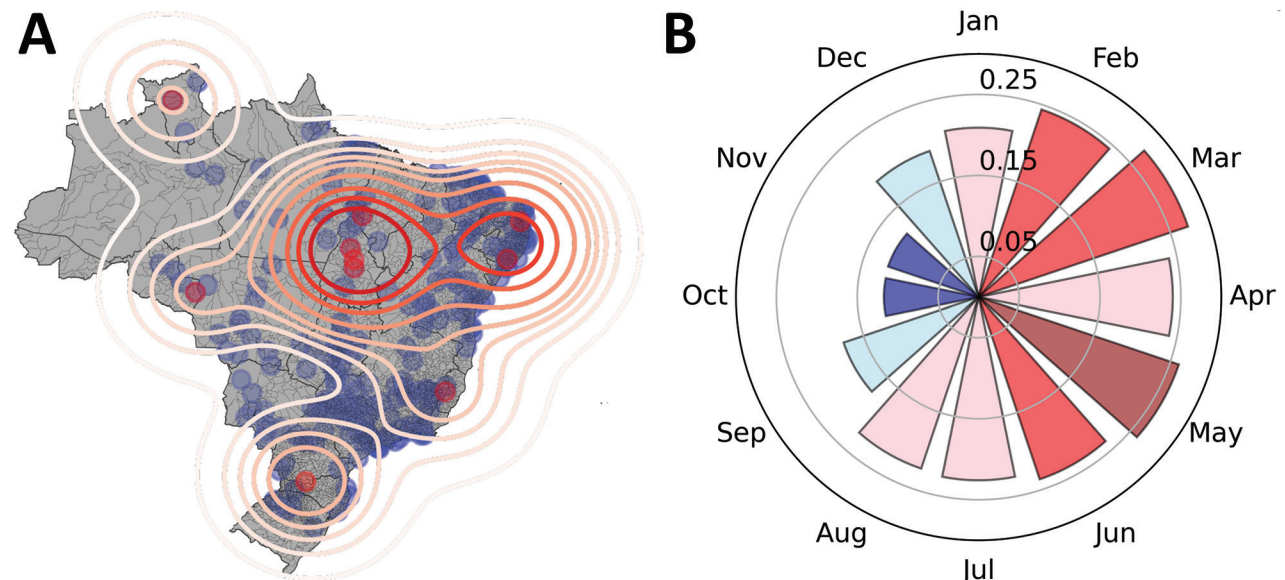


Figure 2. Geographic and temporal distribution of reported Zika cases after the Public Health Emergency of International Concern period, Brazil, 2017–2020. A) Consistency-weighted kernel density estimates. Contours generated with bandwidth determined by Scott's rule adjusted by a factor of 0.7 (12), overlaid on the distribution of all case data. Points show centroids of municipalities that reported infections to the Sistema de Informação de Agravos de Notificação (9) database. B) Monthly Moran I statistic, estimated at the state level. Red indicates $p < 0.05$; blue indicates $p \geq 0.05$.

(Northeast), Rio de Janeiro (Southeast), Paraná (South) and the border between Rondônia (Northern) and Mato Grosso (Central-West).

We calculated the Moran I statistic (13) for infections at the state level to determine significant disease clustering; to do so, we used a permutation approach because of reduced sensitivity to potential violations of the analytical version's assumptions, making it a more robust metric. We calculated a reference distribution for the statistic under the null hypothesis of spatial randomness by randomly permuting the observed values over the locations. We computed Moran I for each randomly shuffled dataset; from the statistic, we plotted a reference distribution and a pseudo p value. Because of the high number of municipalities in Brazil with missing data, we estimated global clustering at the state level. Distrito Federal is contained entirely within the state of Goiás, and so data on its cases and population were merged with Goiás. We estimated a Moran I of 0.23; Monte Carlo simulation generated pseudo p value was 0.047, providing support for clustering at this level (Appendix Figure 7). We then assessed clustering for each calendar month (e.g., we included cases from January 2017, January 2018, January 2019, and January 2020 as Jan) (Figure 2, panel B). Monthly Moran I showed clustering persisting throughout much of the year (January–August) but breaking down when case numbers naturally waned during the low mosquito season (September–December).

Conclusions

The objectives of this study were to identify current trends in ZIKV transmission in Brazil and to identify where, and when throughout the year, ZIKV is most consistently reported in the post-PHEIC period. Limitations of this analysis include the high rates of underreporting known to occur for ZIKV infections which, coupled with difficulties in differential diagnosis, make reliable estimates for case numbers a considerable challenge (14). Because of these uncertainties, the forecasts in our analysis should not be viewed as prescriptive predictions of the true numbers of ZIKV infections in Brazil 2021–2022. Instead, forecasts are estimates for cases that will be reported to the notifiable diseases information system; these forecasts have the potential to accelerate public health decisions informed by the information system.

After validating the SARIMA models fitted to monthly regional notification data from Brazil, we forecasted 8,476 new cases for 2021–2022 (95% CI 279–54,732 new cases). Although the Northeast and Southeast regions were likely to continue to have

the highest total infection numbers, our consistency-weighted, population-standardized rates highlighted hotspot states within all 5 regions. In the national health system, strategic programs are coordinated and specialized services are delivered at the state level; our results can help inform specific municipalities within hotspot states that exhibit consistently high-level notifications. Identifying hotspots has 2 purposes: first, it provides targets for more intensive vector control efforts to ameliorate disease burden among the worst-affected populations; second, it helps to inform site selection for seroprevalence studies and intervention trials (15). Temporality of clustering statistics indicating clear and consistent transmission seasonality also contributes to both of these purposes.

About the Author

Dr. Yakob is an associate professor of infectious diseases at the London School of Hygiene & Tropical Medicine. He uses computational approaches to help target and strategize disease control.

References

1. Yakob L, Walker T. Zika virus outbreak in the Americas: the need for novel mosquito control methods. *Lancet Glob Health*. 2016;4:e148–9. [https://doi.org/10.1016/S2214-109X\(16\)00048-6](https://doi.org/10.1016/S2214-109X(16)00048-6)
2. European Centre for Disease Prevention and Control. Rapid risk assessment: microcephaly in Brazil potentially linked to the Zika virus epidemic. Stockholm: European Centre for Disease Prevention and Control; 2015.
3. Hay JA, Nouvellet P, Donnelly CA, Riley S. Potential inconsistencies in Zika surveillance data and our understanding of risk during pregnancy. *PLoS Negl Trop Dis*. 2018;12:e0006991. <https://doi.org/10.1371/journal.pntd.0006991>
4. Fischer C, Drosten C, Drexler JF. The difficulties in obtaining reliable Zika virus diagnostics. *Lancet Infect Dis*. 2019;19:240–1. [https://doi.org/10.1016/S1473-3099\(19\)30049-0](https://doi.org/10.1016/S1473-3099(19)30049-0)
5. Moore SM, Oidtman RJ, Soda KJ, Siraj AS, Reiner RC Jr, Barker CM, et al. Leveraging multiple data types to estimate the size of the Zika epidemic in the Americas. *PLoS Negl Trop Dis*. 2020;14:e0008640. <https://doi.org/10.1371/journal.pntd.0008640>
6. US Centers for Disease Control and Prevention. Zika in the US. 2021 [cited 2022 Feb 16]. <https://www.cdc.gov/zika/geo/index.html>
7. Pan American Health Organization. PLISA health information platform for the Americas. 2021 [cited 2022 Feb 16]. <https://www3.paho.org/data/index.php>
8. World Health Organization. Prioritizing diseases for research and development in emergency contexts. 2021 [cited 2022 Feb 16]. <https://www.who.int/activities/prioritizing-diseases-for-research-and-development-in-emergency-contexts>
9. Health Surveillance Secretariat of the Ministry of Health. Information about SINAN (Sistema Informação Agravos Notif. e RESP (Registro Eventos Saúde Pública)

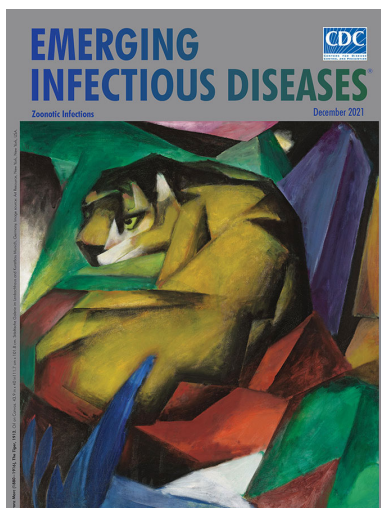
- [in Portuguese]. Brazil; 2016 [cited 2022 Feb 16]. <http://portalsinan.saude.gov.br>
- Rosenblatt M. Remarks on some nonparametric estimates of a density function. *Ann Math Stat.* 1956;27:832–7. <https://doi.org/10.1214/aoms/1177728190>
 - Instituto Brasileiro de Geografia e Estatística. Study on the Continuous Population Census Modality. Brazil: The Institute; 2020.
 - Moran PAP. Notes on continuous stochastic phenomena. *Biometrika.* 1950;37:17–23. <https://doi.org/10.1093/biomet/37.1-2.17>
 - O'Reilly KM, Lowe R, Edmunds WJ, Mayaud P, Kucharski A, Eggo RM, et al. Projecting the end of the Zika virus epidemic in Latin America: a modelling analysis. *BMC Med.* 2018 Oct 3;16:180.
 - World Health Organization. Efficacy trials of ZIKV vaccines: endpoints, trial design, site selection. Meeting report. Geneva: World Health Organization; 2017.
 - Scott DW. Multivariate density estimation: theory, practice, and visualization. New York, NY: John Wiley & Sons; 1992.

Address for correspondence: Laith Yakob, Faculty of Infectious and Tropical Diseases, London School of Hygiene & Tropical Medicine, London, WC1E 7HT, UK; email: laith.yakob@lshtm.ac.uk

December 2021

Zoonotic Infections

- Clinical Characteristics of *Corynebacterium* Bacteremia Caused by Different Species, Japan, 2014–2020
- Evaluation of Early Warning, Alert and Response System for Ebola Virus Disease, Democratic Republic of the Congo, 2018–2020
- Coronavirus Disease Contact Tracing Outcomes and Cost, Salt Lake County, Utah, USA, March–May 2020
- Transmission of Severe Acute Respiratory Syndrome Coronavirus 2 in Households with Children, Southwest Germany, May–August 2020
- SARS-CoV-2 Seroprevalence in a Rural and Urban Household Cohort during First and Second Waves of Infections, South Africa, July 2020–March 2021
- Human Melioidosis Caused by Novel Transmission of *Burkholderia pseudomallei* from Freshwater Home Aquarium, United States
- Trends in Incidence and Clinical Outcomes of *Clostridioides difficile* Infection, Hong Kong
- Characterization of Swine Influenza A(H1N2) Variant, Alberta, Canada, 2020
- Surface–Aerosol Stability and Pathogenicity of Diverse Middle East Respiratory Syndrome Coronavirus Strains, 2012–2018
- Novel Use of Capture–Recapture Methods to Estimate Completeness of Contact Tracing during an Ebola Outbreak, Democratic Republic of the Congo, 2018–2020



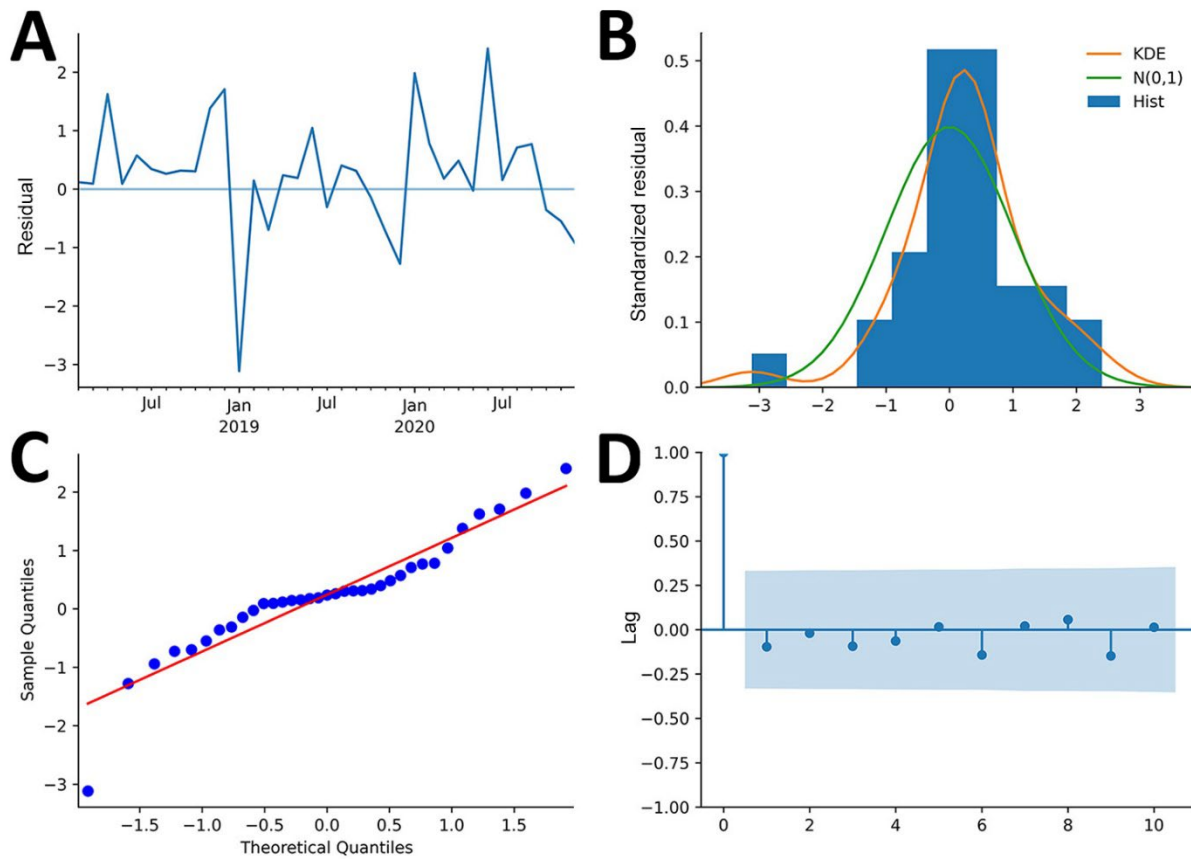
- Novel Filoviruses, Hantavirus, and Rhabdovirus in Freshwater Fish, Switzerland, 2017
- Mammarenaviruses of Rodents, South Africa and Zimbabwe
- Potential Use for Serosurveillance of Feral Swine to Map Risk for Anthrax Exposure, Texas, USA
- SARS-CoV-2–Specific Antibodies in Domestic Cats during First COVID-19 Wave, Europe
- Detection of SARS-CoV-2 in Wastewater at Residential College, Maine, USA, August–November 2020
- Increased Incidence of Melioidosis in Far North Queensland, Queensland, Australia, 1998–2019
- Novel Assay to Measure Seroprevalence of Zika Virus in the Philippines
- Large-Scale Screening of Asymptomatic Persons for SARS-CoV-2 Variants of Concern and Gamma Takeover, Brazil
- Heartland Virus Transmission, Suffolk County, New York, USA
- SARS-CoV-2 Variants, South Sudan, January–March 2021
- Incidence Trends for SARS-CoV-2 Alpha and Beta Variants, Finland, Spring 2021
- Potential Mosquito Vectors for Shuni Virus, South Africa, 2014–2018
- Incubation Period for Neuroinvasive Toscana Virus Infections
- Uptake, Retention, and Excretion of Infectious Prions by Experimentally Exposed Earthworms
- Rift Valley Fever Virus Seroprevalence among Humans, Northern KwaZulu–Natal Province, South Africa, 2018–2019
- Surge of Typhoid Intestinal Perforations as Possible Result of COVID-19–Associated Delays in Seeking Care, Madagascar
- Evidence of Human Exposure to Tamdy Virus, Northwest China
- SARS-CoV-2 B.1.1.7 Variant Infection in Malayan Tigers, Virginia, USA
- Postmortem Stability of SARS-CoV-2 in Mouse Lung Tissue
- Guillain–Barré Syndrome Associated with COVID-19 Vaccination

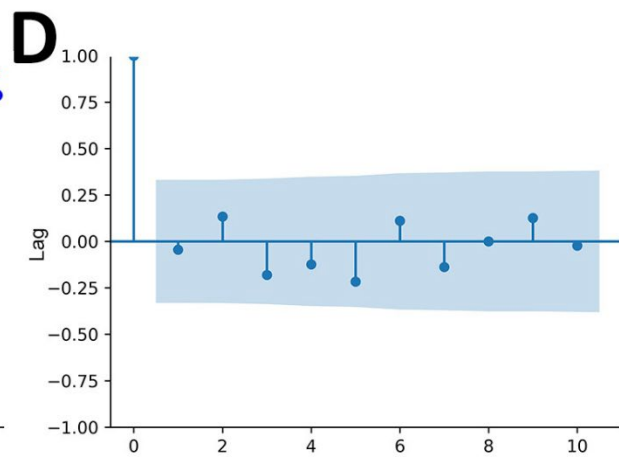
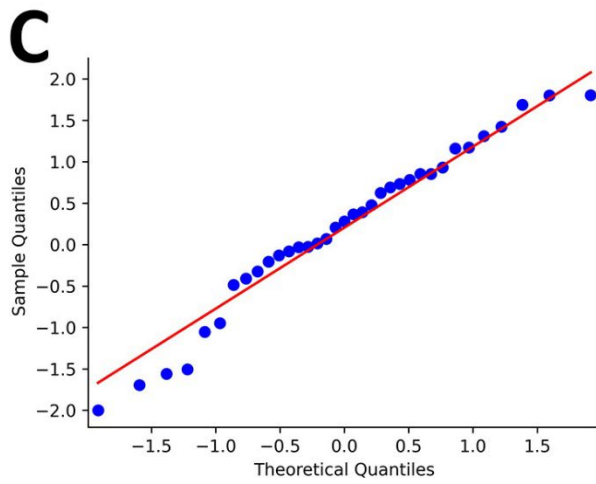
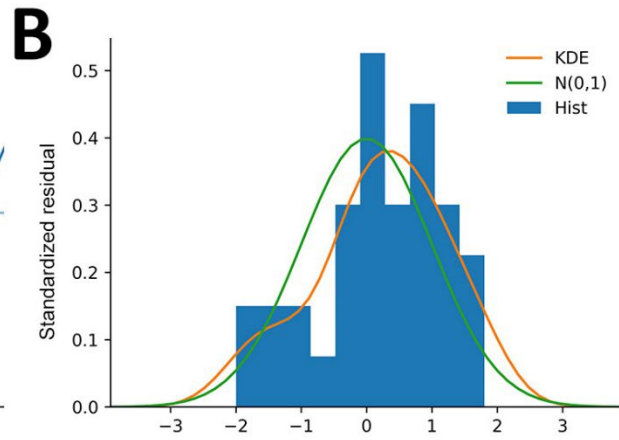
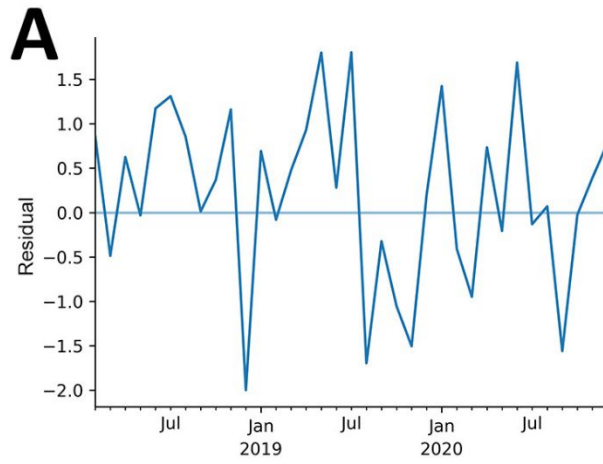
**EMERGING
INFECTIOUS DISEASES**

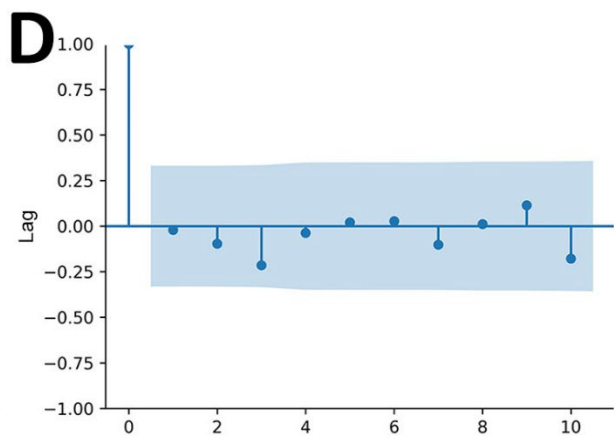
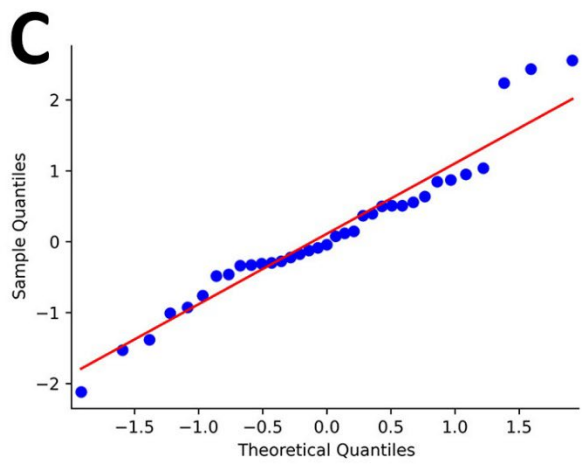
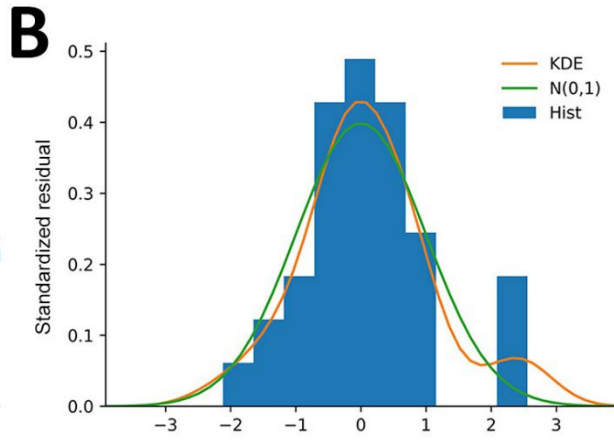
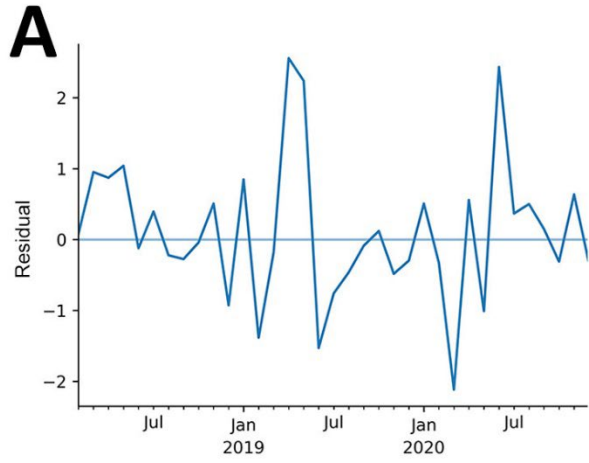
To revisit the December 2021 issue, go to:
<https://wwwnc.cdc.gov/eid/articles/issue/27/12/table-of-contents>

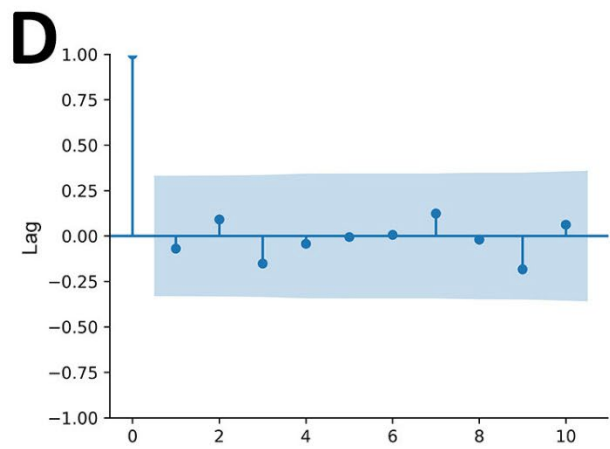
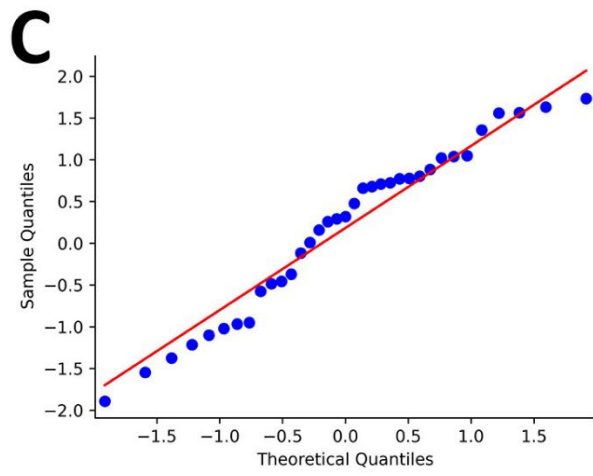
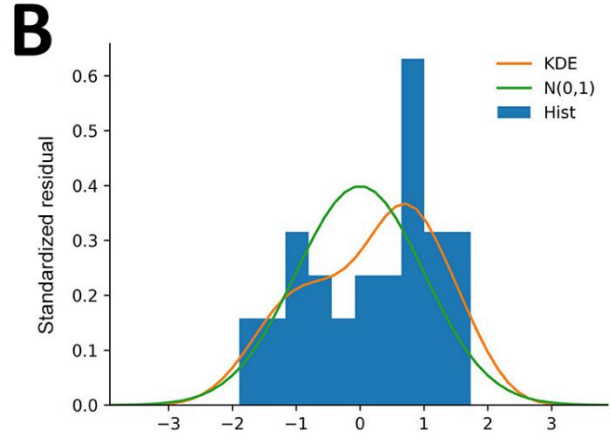
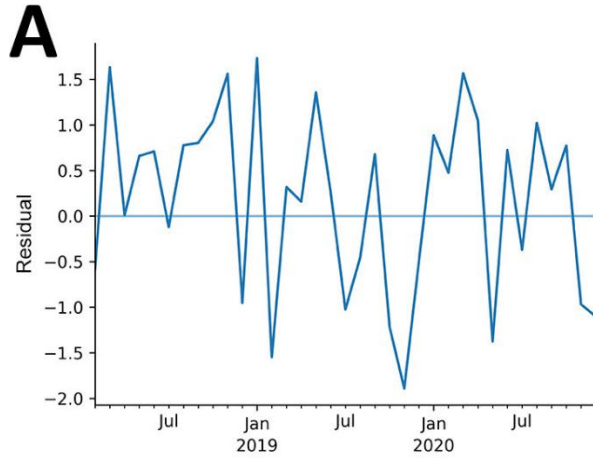
Zika Virus after the Public Health Emergency of International Concern Period, Brazil

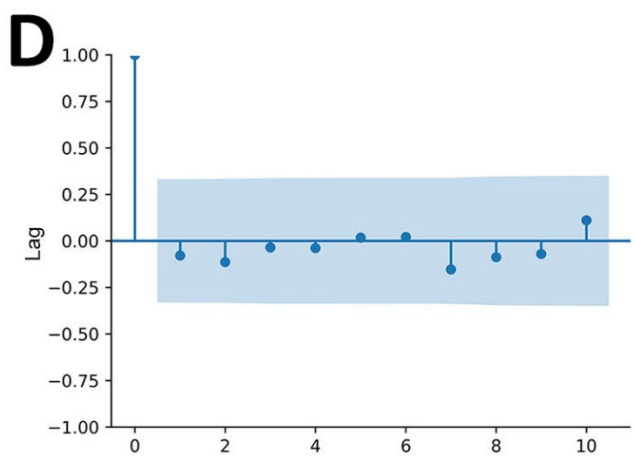
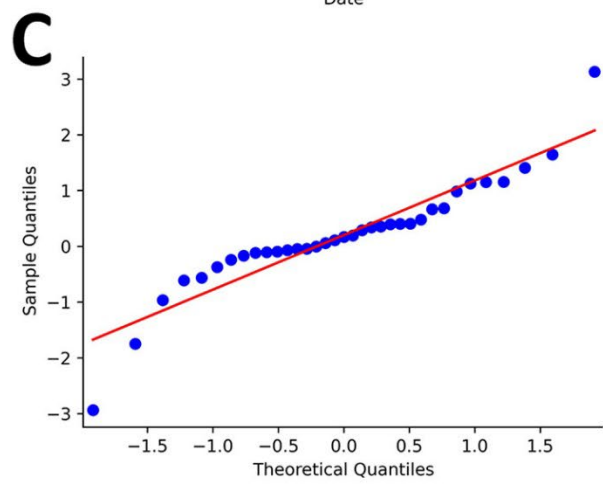
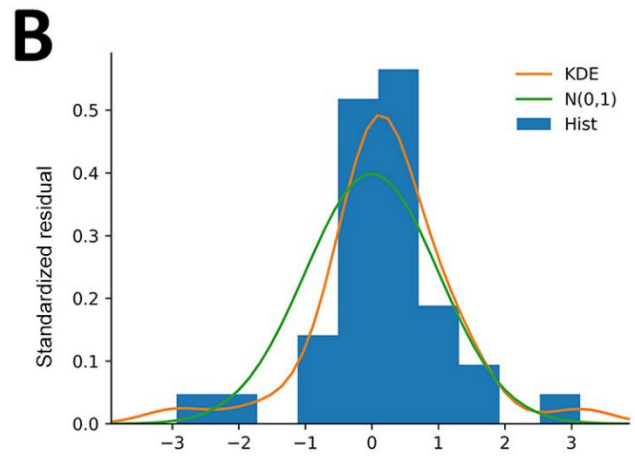
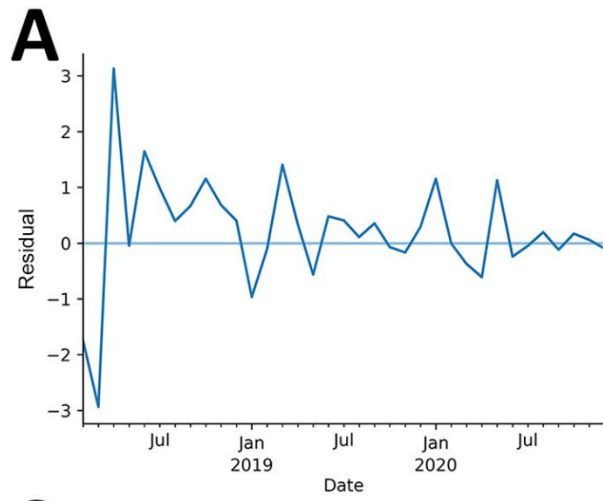
Appendix

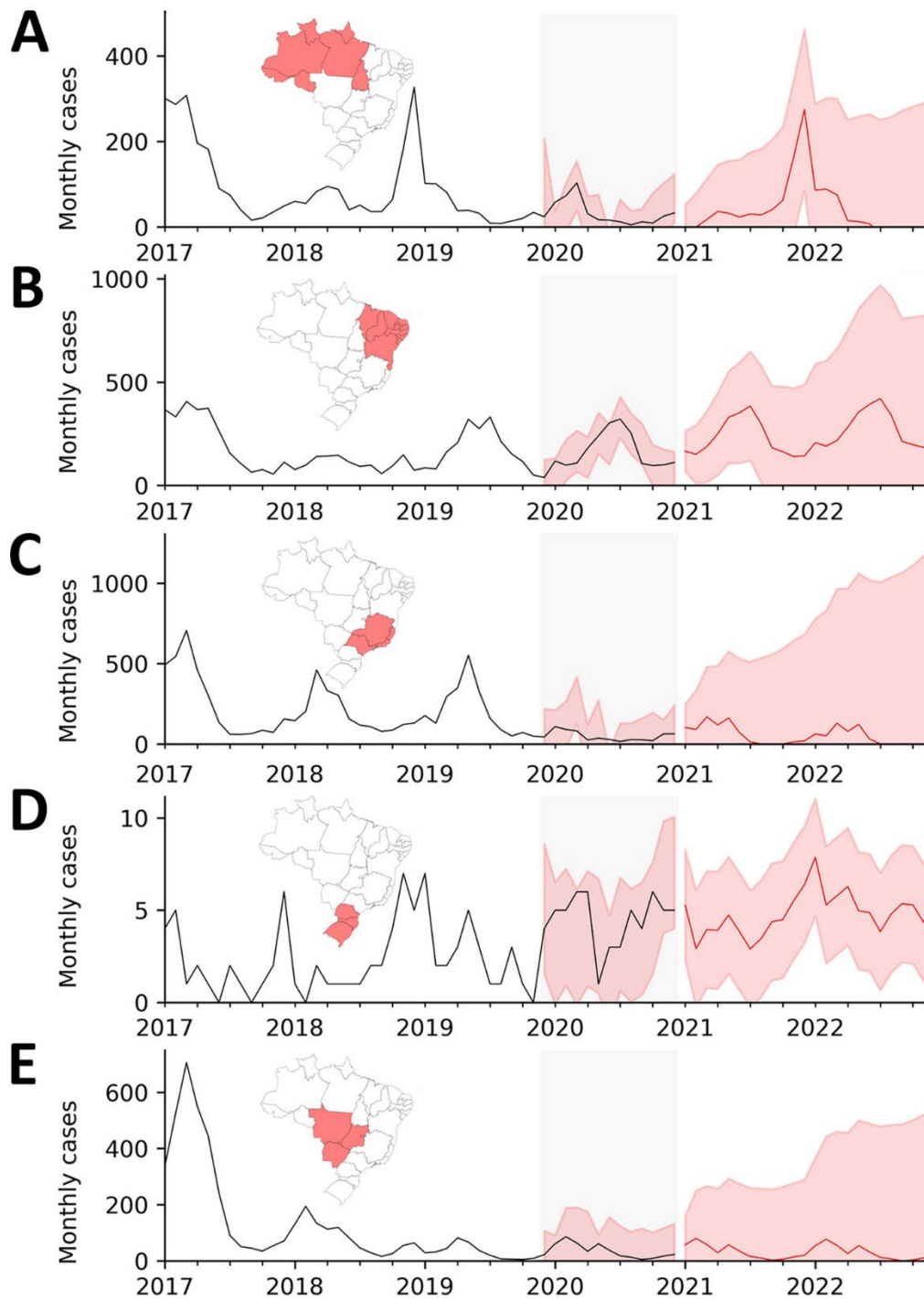












Appendix Figure 6. Seasonal autoregressive integrated moving average (SARIMA) models for Brazil's 5 regions: North (A), Northeast (B), Southeast (C), South (D), Central-West (E). Models were trained with SINAN data up until end of 2019, then validated before forecasting for 2021 and 2022. Gray shading indicates validation period. Black line indicates mean in validation period; red line indicates forecasting mean. Red shading indicates confidence bounds. Diagnostic plots show good SARIMA model fits.

